Available online at www.sciencedirect.com
ScienceDirect
Journal of Molecular Graphics and Modelling 26 (2007) 613–621
Journal of Molecular Graphics and Modelling
www.elsevier.com/locate/JMGM

The photodissociation of ozone: A quasi-classical approach to a quantum dynamics problem

Thomas J. Penfold, Graham A. Worth *

School of Chemistry, University of Birmingham, Edgbaston, Birmingham B15 2TT, UK

Accepted 29 January 2007
Available online 3 February 2007

Abstract

It is extremely difficult to execute full quantum dynamics calculations on complex systems (more then three degrees of freedom) due to the exponential increase in computer resources required by these methods. Classical mechanics simulations do not suffer from this problem, but are unable to treat quantum mechanical phenomena such as non-adiabatic effects, which often play a vital role in photochemical processes. A method has been implemented for carrying out dynamical calculations using quasi-classical theory. The time dependent Schrödinger equation is solved using a swarm of trajectories treated under Newtonian laws and Tully's fewest switches trajectory surface hopping is applied to implement the surface switches. The method was applied to ozone, looking at the photodissociation that takes place after excitation into the Chappuis band of the absorption spectrum. While the goal is to treat larger systems, comparison can be made for ozone with numerically exact wavepacket calculations. The method proved successful at calculating quantities such as the rate of population transfer, but there were discrepancies in the details, especially when surface switching occurred from the lower state.

Keywords: Ozone photodissociation; Wavepacket dynamics; Conical intersections; Trajectory surface hopping; Quasi-classical dynamics

1. Introduction

Molecular dynamics calculations have allowed users to obtain detailed information about a wide range of chemical, biological and physical reactions. These calculations use a variety of different methods ranging from fully quantum dynamical to entirely classical [1]. A dynamical system is represented by a wavepacket, an initial non-stationary wavefunction that evolves with time according to the time-dependent Schrödinger equation. Quantum dynamics calculations solve this equation directly. The problem is that they suffer from an exponential increase in computer resources required, and in their standard form they are limited effectively to systems of three or four atoms. In contrast, trajectory based methods that rely on classical mechanics can treat many thousands of atoms. Classical methods, however, are unable to account for the significant quantum effects that arise from complications such as the breakdown of the Born–Oppenheimer Approximation (BOA) [2,3].

The breakdown of the BOA leads to features such as avoided crossings and conical intersections, regions where potential energy surfaces are close together and the coupling of the nuclear and electronic motion allow the wavepacket to move over more than one surface. [1,2]. Quasi-classical methods, such as those developed by Tully [3] and Truhlar [4], are designed to simulate systems where non-adiabatic effects are known to be important. They can deal with over 1000 degrees of freedom [5] and such methods are obviously attractive for large systems. However, limitations with these methods are well known (see refs. [6,7] for comparisons of different methods). There are fundamental limitations that arise from the basic assumptions of the method: quantum mechanical behaviour of the nuclei is accounted for when changing electronic state, but neglected within a state. Quantum effects such as tunnelling, interference and level quantisation can be significant and thus the methods based upon classical rules are no longer able to replicate experimental observed values [3].

Using the photodissociation of ozone as an example, the aim of the work described in this paper is to implement and test the

* Corresponding author.
E-mail address: g.a.worth@bham.ac.uk (G.A. Worth).

1093-3263/$ – see front matter © 2007 Elsevier Inc. All rights reserved.
doi:10.1016/j.jmgm.2007.01.012

accuracy of a trajectory-based method against accurate quantum dynamic calculations performed by the multi-configuration time-dependent Hartree (MCTDH) [8–10]. This is a powerful wavepacket propagation algorithm that has been used successfully to describe the non-adiabatic dynamics of a number of small molecules [11]. The method implemented is a straightforward application of swarms of trajectories and trajectory surface hopping (TSH) [3]. It is the first stage to including such calculations into the MCTDH package [12] to enable a better comparison of quasi-classical and wavepacket methods.

The reason for this is that we would like to be able to study non-adiabatic systems that are larger than those amenable to present standard quantum dynamics methods. Using the MCTDH method the upper limit is presently 12 atoms, impressive but still far away from the polyatomic molecules of interest in the majority of photochemistry. The comparison with quasi-classical methods will help the development of approximate methods based on MCTDH by focusing on the important features of these systems, and by highlighting what error is introduced by approximations made.

Ozone represents a suitable testing system. It contains three degrees of freedom, and full quantum dynamics calculations are possible. With the strongly coupled excited states there are significant quantum processes testing our classical model, and how well the method describes these will be seen from the comparison of full quantum and quasi-classical propagations. The photodisso-ciation of ozone is a photochemically vital process; the UV photodissociation of O_3 plays a major role in atmospheric oxidation, which prevents harmful solar radiation from reaching the earth's surface [13–15]. The suitability for ozone for preventing harmful radiation from space resides in the weak nature of the O_2–O bond [16]. An average bond strength of 445 kJ mol^{-1} means that radiation with a wavelength <1180 nm has energy above the required activation energy.

Two pathways are important in the bond-breaking

$$O_3(X^1A_1) + h\nu \rightarrow O(2p, {}^1D_2) + O_2(a, {}^1\Delta_g) \quad (1)$$

$$O_3(X^1A_1) + h\nu \rightarrow O(2p, {}^3P_j) + O_2(X, {}^3\Sigma_g{}^-) \quad (2)$$

Eq. (2) is direct dissociation from the ground-state of ozone ending with the oxygen molecule and atom in their ground-states, while the pathway of Eq. (1) is via an excited-state of ozone, leaving both moieties in an excited state.

In the Chappuis band between 400 and 750 nm, excitation takes place to the 1^1A_2 and the 1^1B_1 [13] excited states of ozone. These states are coupled, with a conical intersection providing a fast relaxation pathway from the upper, 1^1B_1, to the lower, 1^1A_2, state. Detailed theoretical analysis of the surfaces and dynamics has been made by Domcke, Schinke and co-workers [17,16,18]. The work finds a repulsive 1^1A_2 surface and a bound 1^1B_1 surface. Excitation to the 1^1B_1 state is thus funnelled into the conical intersection, leading directly into the lower state. Rapid dissociation takes place on the lower surface, corresponding to Eq. (1), with a timescale of approximately 60 fs, leading to a highly diffuse and complex absorption spectrum [13,16,19,20].

2. Theory and computational details

2.1. Potential energy surfaces

The states of interest in the photodissociation of ozone are the 1^1A_2 and the 1^1B_1. Potential energy surfaces and transition dipole moments for these states, and the ground-state were those of Woywod et al. [17]. These are in a diabatic representation provided by a spline-fit to calculated points with a correction factor to give the desired asymptotic behaviour. In a diabatic representation the kinetic energy operator is diagonal and the couplings between states appear as potential-type terms on the off diagonal [2]. The diabatic states can be related to a particular electronic configuration, i.e. a ''chemical character''.

The system is described using Jacobi coordinates so that the cross-terms in the kinetic energy disappear. Ozone has three modes. The vibrational, R_v, mode is one O–O bond. The dissociative, R_d, coordinate joins the third O to the centre-of-mass of the R_v bond. Th angle, θ, then describes the angle between the dissociative mode and the vibrational mode. The ground-state equilibrium values for these mode are 3.21 a.u., 2.46 a.u. and 136.9°, respectively. When the bond angle is 60° or 119.4° a conical intersection is present between the two states [21]. At 119.4° the intersection is close to the Franck–Condon point with an O–O bond length of $R_v \approx 2.45$ a.u.

For the trajectory surface hopping an adiabatic representation was used. The adiabatic states are obtained from the diabatic ones by diagonalisation of the potential operator matrix [2]. In contrast to the diabatic states, these are simply ordered in energy at a particular geometry. Couplings appear in the Hamiltonian as off-diagonal momentum-type terms. The non-adiabatic coupling required to provide the electronic state populations, Eq. (9), are provided by the couplings in the diabatic representation.

2.2. Swarm of trajectories

Bohm's reformulation of quantum mechanics [22,23] used a polar representation for the wavefunction, χ as a function of a real amplitude, A, and phase, S:

$$\chi(R) = A(R)\, e^{(i/\hbar S(R))} \quad (3)$$

where R are the nuclear coordinates. In the classical limit when $\hbar \rightarrow 0$, the time-dependent Schrödinger equation in terms of A and S can then be compared to the equation for fluid flow relating the density, ρ, to the current $\mathbf{J}$:

$$\dot{\rho} + \nabla.\mathbf{J} = 0 \quad (4)$$

where $\bigtriangledown$ is the usual derivative operator with respect to the nuclear coordinates. Using the relationship between the current and the velocity field

$$\mathbf{J} = \rho\mathbf{v} \quad (5)$$

we can obtain the relationship for a set of pseudo-particles in the fluid driven by the potential energy, V

$$m\mathbf{v} = -\nabla V \quad (6)$$

i.e. in the classical limit the wavepacket can be approximated by a swarm of trajectories using classical laws [1].

A particle that can be described by a classical trajectory has a definite position, x, and momenta, p, and therefore is represented as a point in phase space, a representation that the uncertainty principle makes impossible in the quantum picture. Using the Wigner transformation [24], however, the wavefunction that appears in the Schrödinger equation may be transformed to something analogous to a probability distribution in phase space

$$P(x, p) = \frac{1}{\pi\hbar}\int_{-\infty}^{\infty} \mathrm{d}y\, \psi^*(x+y)\psi(x-y)\, \mathrm{e}^{(2ipy/\hbar)} \tag{7}$$

For a harmonic oscillator of mass m and frequency ω at 0 K, the distribution is

$$P(x, p) = \frac{1}{2\pi\hbar}\exp\left[-\frac{1}{\hbar\omega}\left(\frac{p^2}{2m}+\frac{m\omega x^2}{2}\right)\right] \tag{8}$$

The Wigner distribution Eq. (8) can be sampled to set up the initial distribution of trajectories to match the quantum wavepacket. The number of trajectories used to represent the wavepacket defines the accuracy of the calculations, this is always in competition with the computing cost that more trajectories require.

2.3. Trajectory surface hopping

When transitions between potential energy surfaces occur the forces experienced by the wavepacket changes, often drastically. Non-adiabatic phenomena mean that it is critical to incorporate such effects into calculations [3]. There are various methods for classical state switching available including the classical electron model developed by Miller et al. and the Ehrenfest method [5]. However these single best trajectory approaches, despite being suitable for some scenarios, cannot satisfy a whole range of physical situations, when branching occurs. Trajectory surface hopping (TSH), used in conjunction with the fewest switches algorithm developed by Tully [3] is the most popular and robust method, having been tested and used extensively, notably by Truhlar and co-workers [4,7,25–29].

TSH works in tandem with the propagation of a swarm of trajectories. Each trajectory moves on a PES, this motion can be interrupted by a sudden switch to another PES, modelling the non-adiabatic transition. The least-switches algorithm notes that the time-evolution of the electronic Schrödinger equation in terms of the coefficients, c_j, of the electronic state functions, ψ_j, can be written

$$i\hbar\dot{c}_k = V_k c_k - i\hbar\sum_j \dot{\mathbf{R}}.\mathbf{d}_{kj}c_j \tag{9}$$

where V_j is the PES of state j, $\dot{\mathbf{R}}$ the nuclear velocities, and $\mathbf{d}_{kj}$ the non-adiabatic coupling between states j and k, the components of which are given by

$$d_{kj,\alpha} = \langle\psi_k|\nabla_\alpha H_{\mathrm{el}}|\psi_j\rangle \tag{10}$$

where H_{el} is the clamped nucleus electronic Schrödinger equation.The probability of switching state during a time-step Δt is expressed as:

$$P_{k\to j} = -\Delta t\frac{\mathrm{d}}{\mathrm{d}t}\ln c_k^2 \tag{11}$$

The PES the trajectory moves over is changed when the probability of switching becomes greater than a randomly generated number [3,4]. In a region of strong coupling, the probability of state switch occurring will become close to 1, resulting in continuous switching. The fewest switches algorithm controls this by minimising the number of state switches while maintaining the correct state population at all time, ensuring an accurate representation.

When the switch occurs from one state to another, the energy gap is rarely zero. It is therefore necessary to rescale the nuclear velocity to account for this. Following Coker [30]:

$$T^{\mathrm{new}} = T^{\mathrm{old}} - \Delta V \tag{12}$$

where ΔV is the change in potential energy due to the hop and T^{old} and T^{new} the kinetic energy before and after. Using the mass-scaled momentum, $\mathbf{P}$, with components

$$P_\alpha = \frac{p_\alpha}{\sqrt{M_\alpha}} \tag{13}$$

this can be written

$$\frac{1}{2}\mathbf{P}_{\mathrm{new}}.\mathbf{P}_{\mathrm{new}} = \frac{1}{2}\mathbf{P}^{\perp}.\mathbf{P}^{\perp} + \frac{1}{2}\mathbf{P}^{\parallel}.\mathbf{P}^{\parallel} - \Delta V \tag{14}$$

where $\mathbf{P}^{\parallel}$ and $\mathbf{P}^{\perp}$ the components of the momentum before the hop parallel and perpendicular to the derivative coupling vector $\mathbf{d}_{kj}$. The momentum after the hop is then given by

$$\mathbf{P}^{\perp}_{\mathrm{new}} = \mathbf{P}^{\perp} \tag{15}$$

$$\mathbf{P}^{\parallel}_{\mathrm{new}} = \Delta^{\parallel}\mathbf{P}^{\parallel} \tag{16}$$

i.e. only the parallel component is scaled. This has been justified by semi-classical arguments and experience [6]. The scaling factor is

$$\Delta^{\parallel} = \sqrt{\frac{T^{\parallel} - \Delta V}{T^{\parallel}}} \tag{17}$$

where $T^{\parallel} = 1/2\mathbf{P}^{\parallel}.\mathbf{P}^{\parallel}$ is the "parallel" kinetic energy. The kinetic energy is thus re-scaled to conserve the total energy.

The algorithm was implemented in a development version of the Heidelberg MCTDH package [12]. The MCTDH package is designed for full quantum dynamical calculations, as a result it required several modifications to enable it to carry out classical dynamical calculations.

2.4. Quantum dynamics

Wavepacket quantum calculations were performed using the MCTDH algorithm, as implemented in the Heidelberg MCTDH package [12]. The MCTDH algorithm solves the

Schrödinger equation for a wavefunction

$$\Psi(R_1 \cdots R_f, t) = \sum_{j_i=1}^{n_i} \cdots \sum_{j_f=1}^{n_f} A_{j_i \cdots j_f}(t) \prod_{\kappa=1}^{f} \varphi_{j_\kappa}^{(\kappa)}(R_\kappa, t) \tag{18}$$

By applying a variational method, this leads to a set of coupled equations for the motion of single particle functions (SPFs), $\{\varphi\}$, and the expansion coefficients A_j. The time dependent SPF are described by a fixed primitive basis set, such as a discrete variable representation (DVR) [31,9]

$$\varphi_{j_\kappa}^{(\kappa)}(R_\kappa, t) = \sum_{l=1}^{N_\kappa} c_{l j_\kappa}^{(\kappa)}(t) \chi_l^{(\kappa)}(R_\kappa) \tag{19}$$

The efficiency of the method is due to the time-dependent basis set that follows the evolving wavepacket while remaining optimally small. This has enabled the program to perform full quantum calculations on systems with up to 24 degrees of freedom [32]. Details of the algorithm and work done can be found in recent reviews [9,11,33].

The R_d and R_v coordinates were both treated using a sine-DVR from 1.8 to 9.0 a.u. with 120 points. The angle θ used a legendre-DVR with 60 points. To cope with the dissociative part of the potential surfaces, cubic complex absorbing potentials (CAPs) were placed along both R_d and R_v starting at 8.0 a.u. Five SPFs were used for each degree of freedom and each state.

3. Results

The quasi-classical alterations were developed and integrated into the MCTDH package. The accuracy of each alteration was initially assessed in conjunction with quantum calculations on simple systems prior to calculations on ozone.

3.1. The absorption spectrum

In the time dependent picture an absorption spectrum is calculated from a Fourier transform of the autocorrelation function:

$$C(t) = \langle \Psi(0) | \Psi(t) \rangle \tag{20}$$

The absorption spectrum of ozone in the Chappuis band has components due to the two states which can be obtained from propagations starting on the two surfaces. Woywod et al. calculated the spectrum using their surfaces, which we use here, and showed that it agreed very well with the experimental one of Mauersberger et al. [34].

In order to compare easily to the quasi-classical calculations, unlike Woywod et al our calculations did not explicitely include the transition dipole moment, but used a simple vertical excitation of the ground-state wavepacket. A comparison was made between the spectra calculated using either the ground-state wavepacket obtained by energy relaxation [35] on the ground-state surface or an appropriate separable Gaussian-like vibrational wavefunction. Little difference was seen and the absorption spectrum from the simple product-function vertical-excitation ozone model is shown in Fig. 1, obtained from an autocorrelation function of 200 fs convoluted with a exponential damping function of 150 fs.

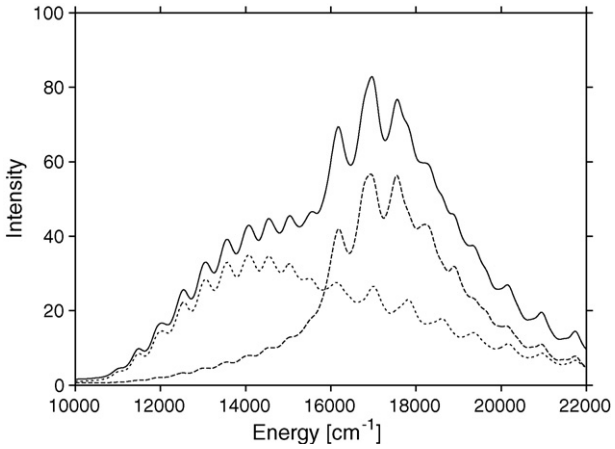

Fig. 1. Calculated absorption spectrum of ozone. The line which peaks at 14,000 cm^{-1} represents the excitation into the 1^1A_2 state, the line which peaks at 17,000 cm^{-1} represents the excitation into the 1^1B_2 state and the bold line is the sum. All spectra are calculated from the Fourier transform of a 200 fs autocorrelation function convoluted with a 150 fs exponential damping function.

The spectrum was calculated using a 1:1 combination of the spectra obtained from the excitation from each of the two states of interest. The lower dissociative state shows a broad band peaking at at 14,000 cm^{-1}, while the upper state shows three major peaks between 16,000, and 18,000 cm^{-1}. Excitation above this level gives a diffuse spectrum with less regular structure. As this is a bound state, the diffuse nature of this band is due to the vibronic coupling. The spectrum is very similar to that of Woywod et al. [16], the major difference being an overestimation of the low energy part of the spectrum due to the 1:1 weighting chosen. The agreement shows that the Condon approximation is reasonable for this system.

3.2. Propagation: photodissociation of ozone

Molecular dynamic calculations using quasi-classical and quantum simulations were performed in the MCTDH package. The kinetic energy operator was the usual Jacobi coordinate operator with zero total angular momentum, $J = 0$. Figs. 2–4 show the relative populations of the excited states of ozone during the first 65 fs of propagation.

Fig. 2 shows the diabatic state populations from the quantum dynamics simulation. Thus this charts the change in electronic character with time. Fig. 2(b) plots the populations starting in the upper 1^1B_1 state. Within 10 fs the state populations are equal and, apart from some small oscillations, the two states essentially remain in parity. This feature indicates the strength of the coupling between the two states. The populations from a propagation initiated on the lower state behaves slightly differently, as shown in Fig. 2(a). Parity between the two states is never reached, and the oscillations observed are larger in the initial femtoseconds. A significant mixing of states is still seen though.

The humps observed in both figures at 40 fs is a reccurance. This feature appears because not all of the wavepacket

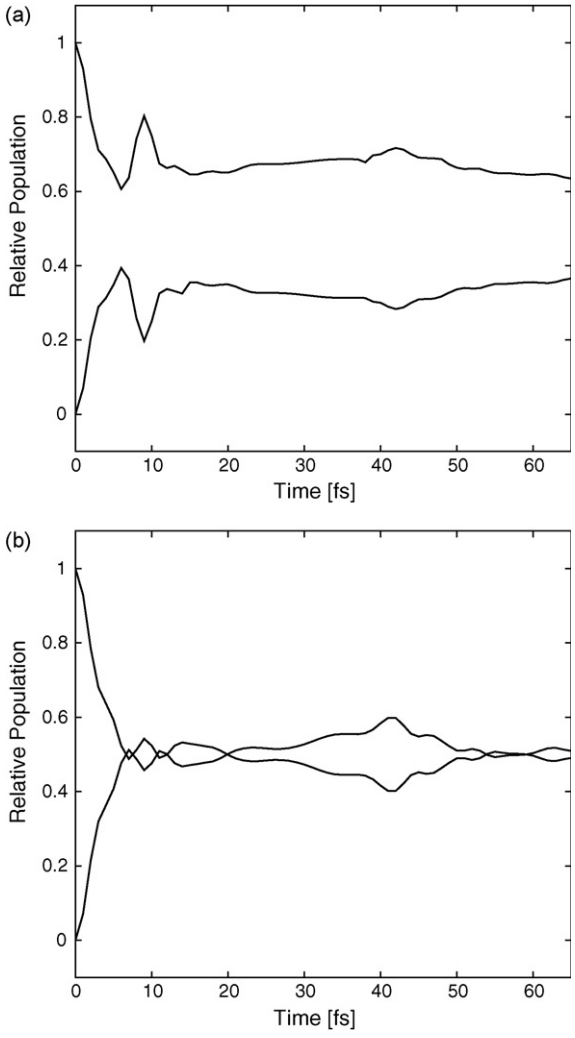

Fig. 2. The diabatic state populations of ozone during the first 65 fs after photo-excitation from the ground-state from a quantum dynamics simulation. (a) Starting from 1^1A_2. (b) Starting from 1^1B_1.

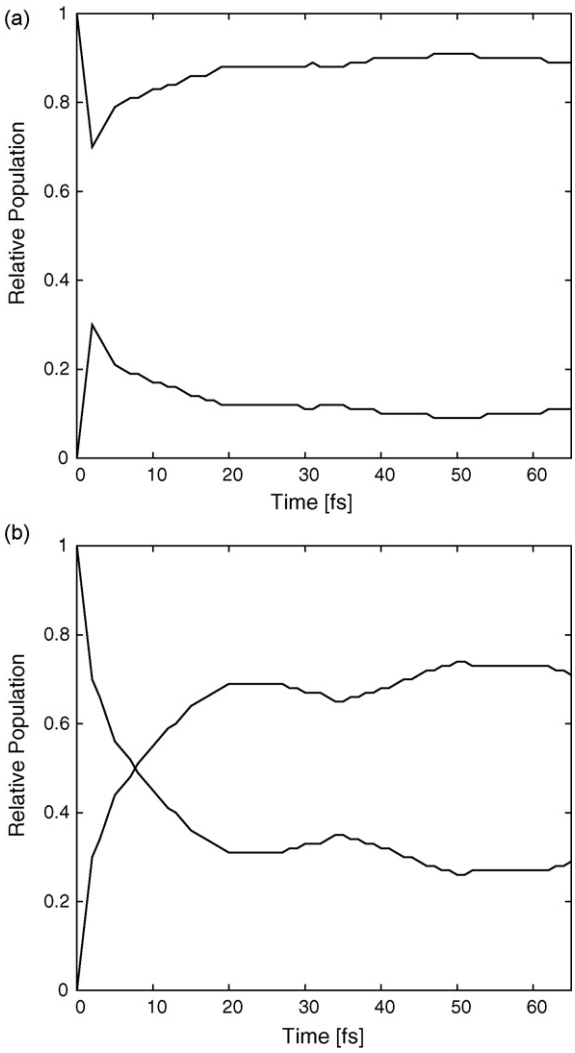

Fig. 3. The adiabatic state populations of ozone during the first 65 fs after photo-excitation from the ground-state from a quantum dynamics simulation. (a) Starting from 1^1A_2. (b) Starting from 1^1B_1.

dissociates immediately [16]. In fact approximately 5% of the overall wavepacket will return of the origin of the propagation and as it re-crosses the non-adiabatic region part of the wavepacket changes state again. Recurrences are seen more clearly in an autocorrelation function and will continue until the density becomes negligible.

Fig. 3 represents the same propagations in the adiabatic representation, obtained from a transformation of the diabatic wavepacket. In Fig. 3(b) the adiabatic populations after starting in the upper diabatic state is plotted. The transfer to the lower surface starts almost immediately, showing that the wavepacket starts out very close to the conical intersection. The transfer is almost over after 20 fs, having transferred 70% of the density. A very different behaviour is seen when starting on the lower surface. Fig. 3(a) shows very little population is transferred: about 20% is transferred at the start of the propagation but the amount drops with time and the system remains almost entirely in the lower state.

The adiabatic populations can be compared directly with the populations obtained from the classical simulation, shown in Fig. 4. These are defined as the percentage of the trajectory swarm in the state at time t. The swarm contained 1000 trajectories, sampling from the Wigner distribution of the separable Gaussian function used for the quantum calculations. Starting in the $^1B_1$ state, the populations are plotted in Fig. 4(b). Comparisons between Figs. 3(b) and 4(b) indicate a reasonable agreement between the two calculations, especially in the intersection region at approximately 10 fs. The quasi-classical trajectories are clearly finding and passing through the conical intersection with around the same time-scale as the quantum calculations. The transfer of population is, however, more – it is all transferred – and slightly faster. The quasi-classical calculations are, however, completely unable to reproduce the population transfer starting in the lower $^1A_2$ state. This is plotted in Fig. 4(a) and in contrast to the quantum calculation in 3(a) an almost negligible state switching is seen in the quasi-classical calculation. What occurs takes place in the correct position though.

It has been proposed that the shortcomings of the classical model can be explained by the absence of coherence and the

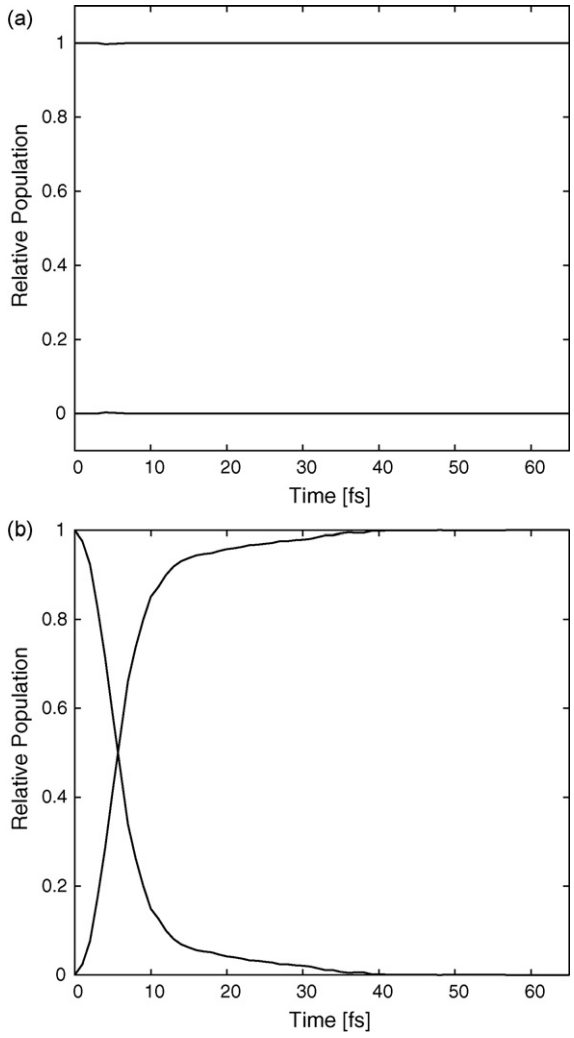

Fig. 4. The adiabatic state populations of ozone during the first 65 fs after photo-excitation from the ground-state from a quasi-classical simulation with 1000 trajectories. (a) Starting from 1^1A_2. (b) Starting from 1^1B_1 trajectories.

strict observation of classical laws in the classical wavepacket (frustrated hops):

- *Absence of coherence*. The quantum wavepacket is coherent throughout, i.e. it moves as a single entity. As a result the state switching of one portion will affect the probability of another section following it onto the new surface. This is not recreated in the classical model because each trajectory acts as an individual entity whose behaviour is independent of its neighbours. Absence of coherence within the wavepacket is also responsible for the inability of the classical model to replicate recurrences.
- *Frustrated hops*. In a quasi-classical simulation the situation can occur when the probability of hopping is large but the change in potential energy is greater then the kinetic energy. This is not allowed, resulting in a frustrated hop. The quantum wavepacket, in contrast, is able to switch from the lower state to the upper state unrestrained by classical mechanics: the total energy must be conserved globally but not locally. This effect is seen strongly in Fig. 4(a). Even when the coupling is very strong (the first 10 fs) the trajectories do not hop. Frustrated hops were also observed, but are less significant, when starting from the 1^1B_1 state.

The population plots of the two states is not sufficient in obtaining a complete picture of the dynamics of the dissociation process. Fig. 6 shows snapshots of the wavepacket motion on the lower adiabatic surface after starting in the upper state. The wavepacket is plotted as the adiabatic density, integrating over the angle coordinate. For the quasi-classical simulations the density was obtained by collecting the trajectories into bins to form a grid. The population transfers in this scenario are in good agreement between the quantum and quasi-classical calculations, as the figure shows. However, significant differences are seen in the actual dynamics. The corresponding plot for the calculations starting in the lower state is less interesting. No population transfer occurs in the quasi-classical calculation so nothing can be said about differences in dynamics after switching state.

Fig. 5 shows the potential energy over which this evolution is occurring. The cut shown is in the space of the R_d and R_v coordinates with the angle kept at $\theta = 120^\circ$. The dissociation channel along R_d is clear, as is the bound well of the vibrational motion. The conical intersection with the upper adiabatic surface is the cause of the narrowing of the transition state plateau at $(R_d, R_v) \approx (3.0, 3.0)$, this compares favourably with literature values, where the more accurate CASPT2 method gives $(R_d, R_v) \approx (2.5, 2.5)$ [17,18].

Looking now at the density in the lower state, in both simulations density appears after 5 fs close to the conical intersection as a tight packet. The packet then spreads out before dissociation occurs on this repulsive surface. In Fig. 6(b) the quantum wavepacket is seen to follow the channels of the potential surface. At 50 fs the wavepacket appears to have split into three parts, one at the intersection, one in the vibrational well, and one dissociating. There is obviously a lot of vibrational energy present as the system is able to move a long way out along the vibrational coordinate.

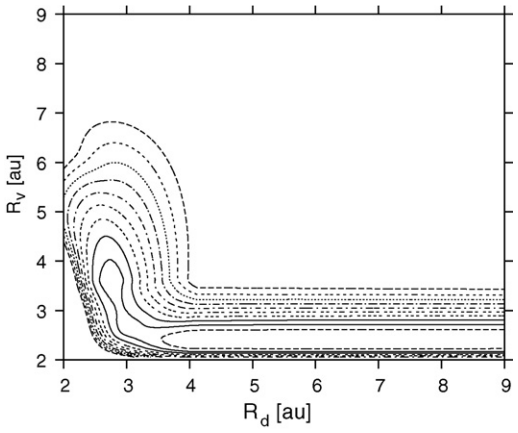

Fig. 5. The lower adiabatic potential energy surface, relating to the 1^1A_2 state of ozone in the space of the R_v and R_d Jacobi coordinates with the angle $\theta = 120^\circ$. Contours are from 0.8 to 3.8 eV. Surface from ref. [17].

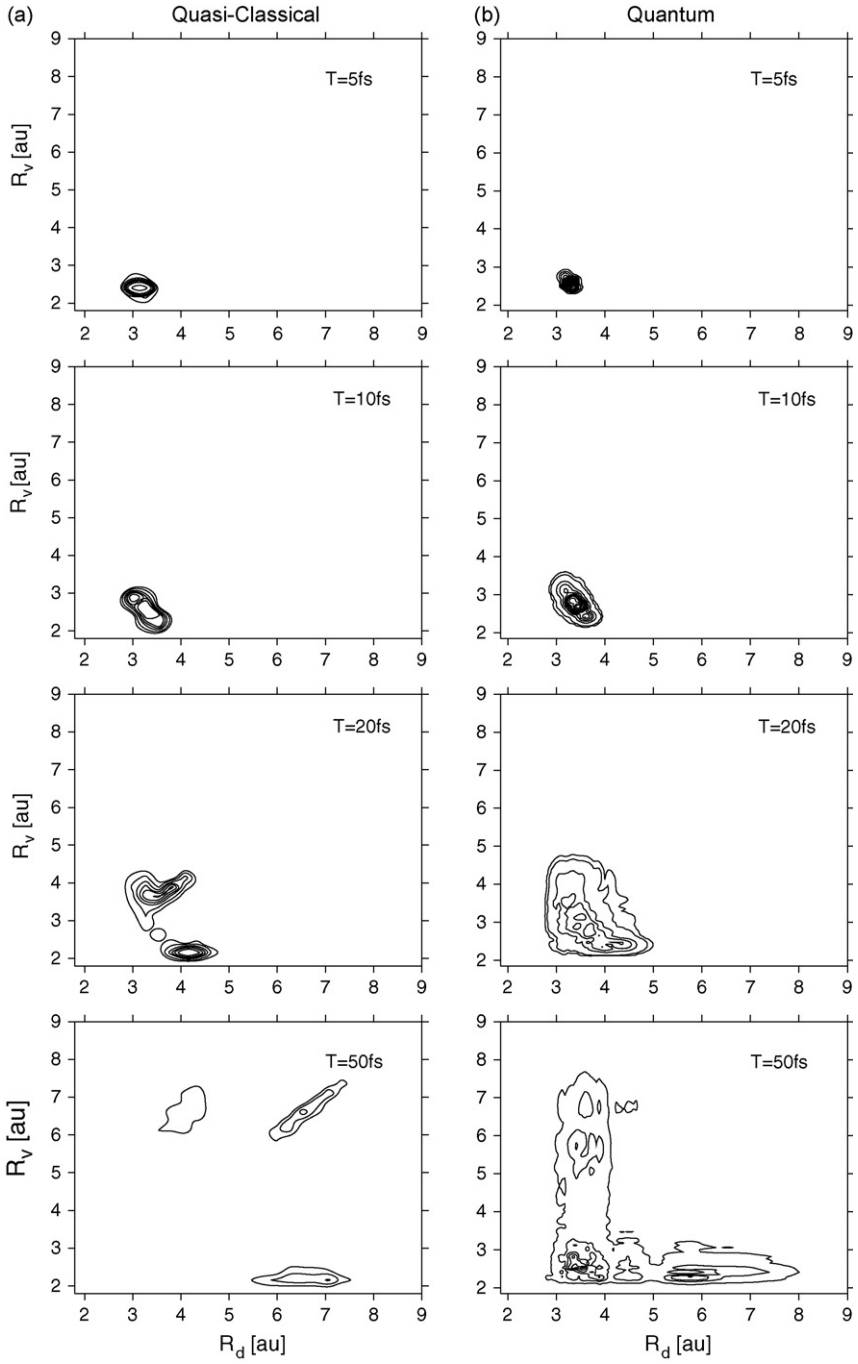

Fig. 6. Snapshots of the wavepacket motion, plotted as the adiabatic density, in the R_d and R_v modes of the lower state starting in the upper diabatic state. (a) Quasi-classical simulation. (b) Quantum dynamics simulation.

The density from the quasi-classical simulation is shown in Fig. 6(a). This shows the same that by 50 fs the wavepacket again has split into a dissociative and a highly excited vibrational part. There is, however, no density left around the intersection, and a new dissociative wavepacket is found along the diagonal, which is in conflict with the potential energy surface where only one dissociative channel exists. This can be attributed to the lack of nuclear coherence, each trajectory acting as a single entity. The energy is thus flowing into both bonds, which should not happen.

4. Conclusion

In this paper a comparison of quantum and quasi-classical dynamics simulations of the photodissociation of ozone in the Chappuis band are compared. The quasi-classical simulation used a swarm of trajectories with Tully's least-switches trajectory surface hopping algorithm and Coker's momentum rescaling factor in order to obtain a classical method for solving non-adiabatic problems.

The simulations propagated wavepackets over the strongly coupled 1^1A_2 (lower) and 1^1B_1 (upper) surfaces using both

methods. Results obtained from propagation beginning in the upper state showed a good agreement between the time-scales of crossing of the quasi-classical and quantum results. The Propagation beginning in the lower state, however, failed to reproduce the quantum behaviour observed, with virtually no switching between the two states, even with the strongly coupled region. These results suggest that although the motion of the wavepacket over a potential energy surface is reasonably replicated, the classical assumptions are unable to reproduce quantum results when certain, subtle, quantum effects are significant. The discrepancies were attributed to the trajectories acting as single entities, compared to the entirely coherent quantum wavepacket, and to the frustrated hops, state switches prevented in the classical model by the conservation of energy.

The plots of the wavepacket motion support the information obtained from the relative population plots. It is clear that the classical wavepacket is unable to recreate the coherence within the quantum wavepacket, resulting in a more dispersed wavepacket, which reduces the probability of switching states at later times. A, perhaps more critical, error due to the trajectories acting as individual classical entities is that the energy flow into both bonds allows a bifurcation of the wavepacket along the $R_v = R_d$ direction, giving a second dissociative channel.

The calculations here are for zero total angular momentum. It could be asked how the agreement would change for higher J states. While further calculations are needed to examine this fully, the results above lead us to expect that, if anything, the agreement will get worse. The error in the quasi-classical calculations is due to a re-distribution of energy that is not allowed quantum mechanically and this will become more of a problem with greater energy.

In summary, a quasi-classical model has been implemented in the MCTDH package, which will allow us to compare it, and modified schemes, to quantum dynamics more easily in the future. Its simple nature provides great advances in terms of the computing cost, allowing more complex systems to be studied in this manner. However, improvements are required to ensure that the classical model is able to accurately reproduce quantum effects, such as switching from a lower state. The problems such as coherence and frustrated hops are being addressed by various groups (see e.g. [28]). An aim must be to keep the simplicity of the algorithm so that the computing cost advantage is negligible.

Acknowledgements

This paper is dedicated to Graham Richards for his 67th birthday in appreciation of his scientific career, his inspirational teaching, and his support and friendship. Thanks are also due to Clemens Woywod for supplying the ozone potential energy surfaces.

References

[1] G.A. Worth, M.A. Robb, Applying direct molecular dynamics to non-adiabatic systems, Adv. Chem. Phys. 124 (2002) 355–432.
[2] G.A. Worth, L.S. Cederbaum, Beyond Born–Oppenheimer: Conical intersections and their impact on molecular dynamics, Ann. Rev. Phys. Chem. 55 (2004) 127–158.
[3] J.C. Tully, Molecular dynamics with electronic transitions, J. Chem. Phys. 93 (1990) 1061.
[4] A.W. Jasper, D.G. Truhlar, Improved treatment of momentum at classically forbidden electronic transitions in trajectory surface hopping, Chem. Phys. Lett. 369 (2003) 60.
[5] K. Drukker, Basics of surface hopping and mixed quantum/classical simulations, J. Comp. Phys. 153 (1999) 225–272.
[6] M.D. Hack, A. Jasper, Y.L. Volobuev, D.W. Schwenke, D.G. Truhlar, Quantum mechanical and quasiclassical trajectory surface hopping studies of the electronically non-adiabatic predissociation of the $\tilde{A}$ state of NaH_2, J. Phys. Chem. A 103 (1999) 6309–6326.
[7] M.S. Topaler, M.D. Hack, T.C. Allison, Y.-P. Liu, S.L. Mielke, D.W. Schwenke, D.G. Truhlar, Validation of trajectory surface hopping methods against accurate quantum mechanical dynamics and semiclassical analysis of electronic-to-vibrational energy transfer, J. Chem. Phys. 106 (1997) 8699–8709.
[8] H.-D. Meyer, U. Manthe, L.S. Cederbaum, The multi-configurational time-dependent Hartree approach, Chem. Phys. Lett. 165 (1990) 73–78.
[9] M.H. Beck, A. Jäckie, G.A. Worth, H.-D. Meyer, The multiconfiguration time-dependent Hartree method: a highly efficient algorithm for propagating wavepackets, Phys. Rep. 324 (2000) 1–105.
[10] H.-D. Meyer, MCTDH Home page: http://www.pci.uni-heidelberg.de/tc/usr/mctdh.
[11] G. Worth, H.-D. Meyer, L. Cederbaum, Multidimensional dynamics involving a conical intersection: wavepacket calculations using the mctdh method, in: W. Domcke, D. Yarkony, H. Köppel (Eds.), Conical Intersections: Electronic Structure, Dynamics and Spectroscopy, World Scientific, Singapore, 2004, pp. 583–617.
[12] G.A. Worth, M.H. Beck, A. Jäckie, H.-D. Meyer, The MCTDH Package, Version 8.3, see http://www.pci.uni-heidelberg.de/tc/usr/mctdh/, 2003.
[13] Z.-W. Qu, H. Zhu, R. Schinke, The ultraviolet photodissociation of ozone revisited, Chem. Phys. Lett. 377 (2003) 359.
[14] G. Barinovs, N. Markovic, G. Nyman III., Wavepacket calculations of ozone photodissociation in the hartley band: convergence of the autocorrelation function, Chem. Phys. Lett. 315 (1999) 282–286.
[15] J.D. Geiser, S.M. Dylewski, J.A. Mueller, R.J. Wilson, R. Toumi, P.L. Houston, The vibrational distribution of O_2 ($x^3\sigma_g^-$) produced in the photodissociation of ozone between 226 and 240 and at 266 nm, J. Chem. Phys. 112 (2000) 1279.
[16] H. Flöthmann, C. Beck, R. Schinke, C. Woywod, W. Domcke, Photodissociation of ozone in the chappuis band II. wavepacket calculations and interpretation of diffuse vibrational structures, J. Chem. Phys. 107 (1997) 7296–7312.
[17] C. Woywod, M. Stengle, W. Domcke, H. Flöthmann, R. Schinke, Photodissociation of ozone in the chappuis band. I. Electronic structure calculations, J. Chem. Phys. 107 (1997) 7282–7294.
[18] S.Y. Grebenschchikov, R. Schinke, Z.-W. Qu, H. Zhu, Absorption spectrum and assignment of the chappuis band of ozone, J. Chem. Phys. 124 (2006) 204313(l)–204313(13).
[19] V.S. Batista, W.H. Miller, Semiclassical molecular dynamics simulations of ultrafast photodissociation dynamics associated with the chappuis band of ozone, J. Chem. Phys. 108 (1997) 498–510.
[20] Y. Chen, L. Hunziker, P. Ludowise, M. Morgen, Femtosecond transient stimulated emission pumping studies of ozone visible photodissociation, J. Chem. Phys. 97 (1992) 2149–2152.
[21] R.L.M.M. Braunstein, P.J. Hay, R.T. Pack, The lowest excited $^1a_2$ and $^1b_1$ states of ozone: two conical intersections and their impact, J. Chem. Phys. 95 (1991) 8239.
[22] D. Bohm, A suggested interpretation of the quantum theory in terms of hidden variables. I., Phys. Rev. 85 (1952) 166–179.
[23] A. Messiah, Quantum Mechanics, vol. 1, John Wiley, New York, 1962.
[24] E. Wigner, Phys. Rev. 40 (1932) 749.
[25] M.D. Hack, A.W. Jasper, Y.L. Volobuev, D.W. Schwenke, D.G. Truhlar, Do semiclassical trajectory theories provide an accurate picture of

radiationless decay for systems with accessible crossings? J. Phys. Chem. A 104 (2000) 217–232.
[26] M.D. Hack, D.G. Truhlar, Non-adiabatic trajectories at an exhibition, J. Phys. Chem. A 104 (2000) 7917–7926.
[27] M.D. Hack, A.M. Wensmann, D.G. Truhlar, M. Ben-Nun, T.J. Martinez, Comparison of full multiple spawning, trajectory surface hopping, and converged quantum mechanics for electronically non-adiabatic dynamics, J. Chem. Phys. 115 (2001) 1172–1186.
[28] M.S. Topaler, T.C. Allison, D.W. Schwenke, D.G. Truhlar, Test of trajectory surface hopping against accurate quantum dynamics for an electronically non-adibatic chemical reaction, J. Chem. Phys. 102 (1998) 1666–1673.
[29] M.S. Topaler, T.C. Allison, D.W. Schwenke, D.G. Truhlar, What is the best semiclassical method for photochemical dynamics of systems with conical intersections? J. Chem. Phys. 109 (1998) 3321–3345.
[30] D.F. Coker, Computer simulation methods for non-adiabatic dynamics in condensed systems, in: M.P. Allen, D.J. Tildesley (Eds.), Computer Simulation in Chemical Physics, Kluwer Academic, Dordrecht, 1993, pp. 315–377.
[31] J.C. Light, T. Carrington Jr., Discrete variable representations and their utilization, Adv. Chem. Phys. 114 (2000) 263–310.
[32] A. Raab, G. Worth, H.-D. Meyer, L.S. Cederbaum, Molecular dynamics of pyrazine after excitation to the S2 electronic state using a realistic 24-mode model Hamiltonian, J. Chem. Phys. 110 (1999) 936–946.
[33] H.-D. Meyer, G.A. Worth, Quantum molecular dynamics: propagating wavepackets and density operators using the multiconfiguration time-dependent Hartree method, Theor. Chem. Ace. 109 (2003) 251–267, feature article.
[34] S.M. Andersson, K. Mauersberger, Ozone absorption-spectroscopy in search of low lying electronic states, J. Geophys. Res. 100 (1995) 3033.
[35] R. Kosloff, H. Tal-Ezer, A direct relaxation method for calculating eigenfunctions and eigenvalues of the Schrödinger equation on a grid, Chem. Phys. Lett. 127 (1986) 223.